Astrobiology
Lecture 15

Exoplanets: detection and characterization

SISSA, Academic Year 2023
Giovanni Vladilo (INAF-OATs)

Detection methods of exoplanets

Direct methods

–Direct imaging of the planet

Indirect methods

- Mostly based on effects induced on the host star

Gravitational perturbation of the stellar motion
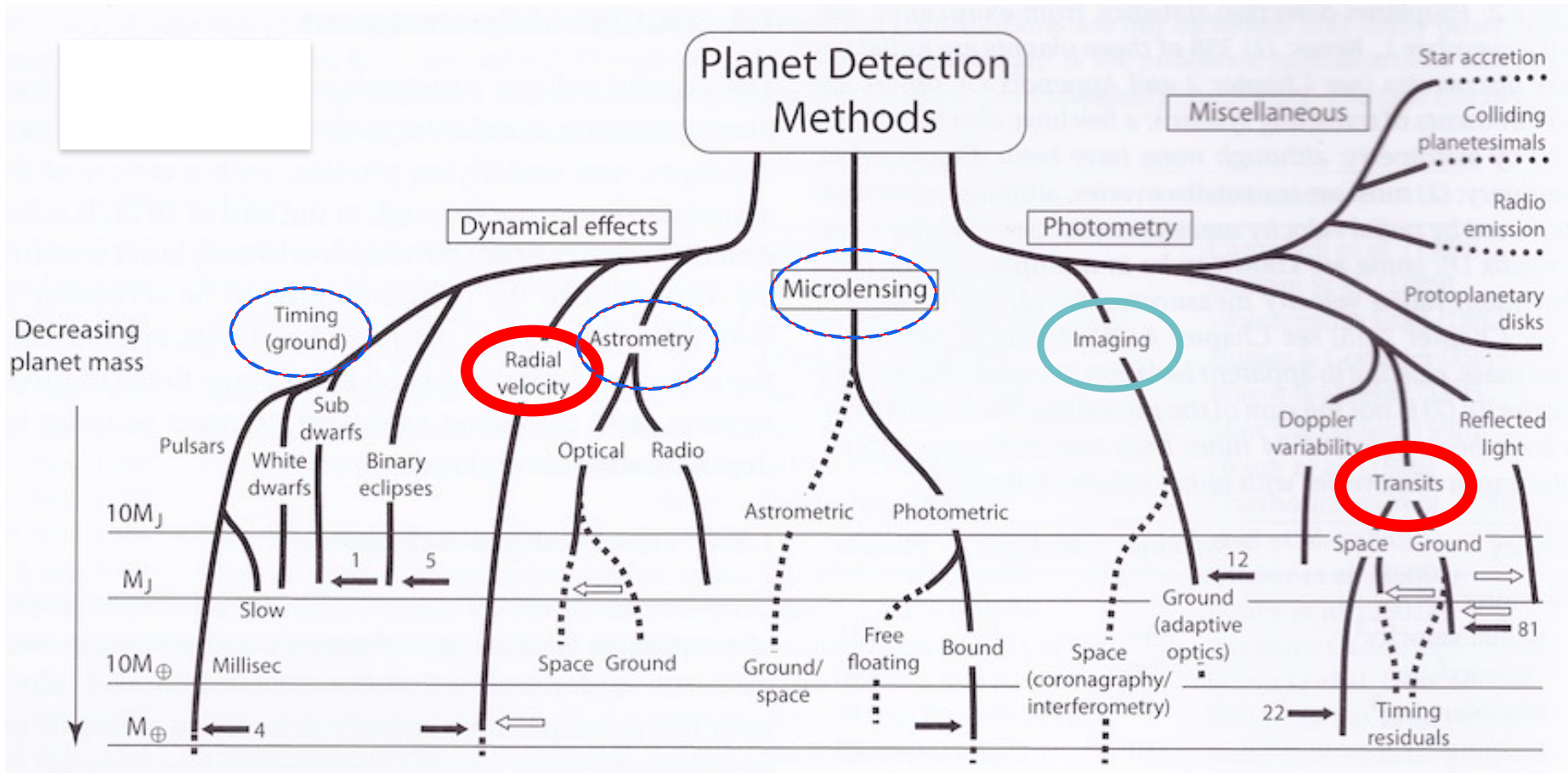
Variations of the stellar luminosity

Immediate goal: derivation of Keplerian orbital parameters

a: semimajor axis

P: orbital period

e: orbital eccentricity

Exoplanet detection methods

Direct imaging: observational challenges

Luminosity contrast

L_p/L_*

– Optical spectral band

  reflected stellar radiation

  varies with the orbital phase

  contrast ~ 10^9-10^{10}

– Infrared spectral band (~10 μm)

  intrinsic planetary emission

  contrast ~ 10^6-10^7

Optical band

$$L_p \sim L_* \left(\frac{R_p}{a}\right)^2 \Phi(t)$$

$$\Phi(t) = 1 - \sin i \sin\left(\frac{2\pi t}{P}\right)$$

Infrared band

$$L_p \sim L_* \left(M_p/M_*\right)$$

Direct imaging: observational challenges

Planet-star angular separation

Angular separations can be estimated as a function of stellar distance, l, and orbital semimajor axis of the planet, a

$$\vartheta = \arctan \frac{a}{\ell}$$

Typical values are lower than 1 arcsec

e.g., the Earth-Sun separation as seen from 20 pc is 50 mas

The luminosity contrast makes hard to attain the theoretical <u>diffraction limit</u> $\delta\vartheta \cong \lambda/D$ (radius of the Airy disk)

   D : telescope diameter

   λ : wavelength of the observations

Direct imaging of exoplanets
Example

GJ 504 b

$M = 4\ M_J$

$a = 44$ AU

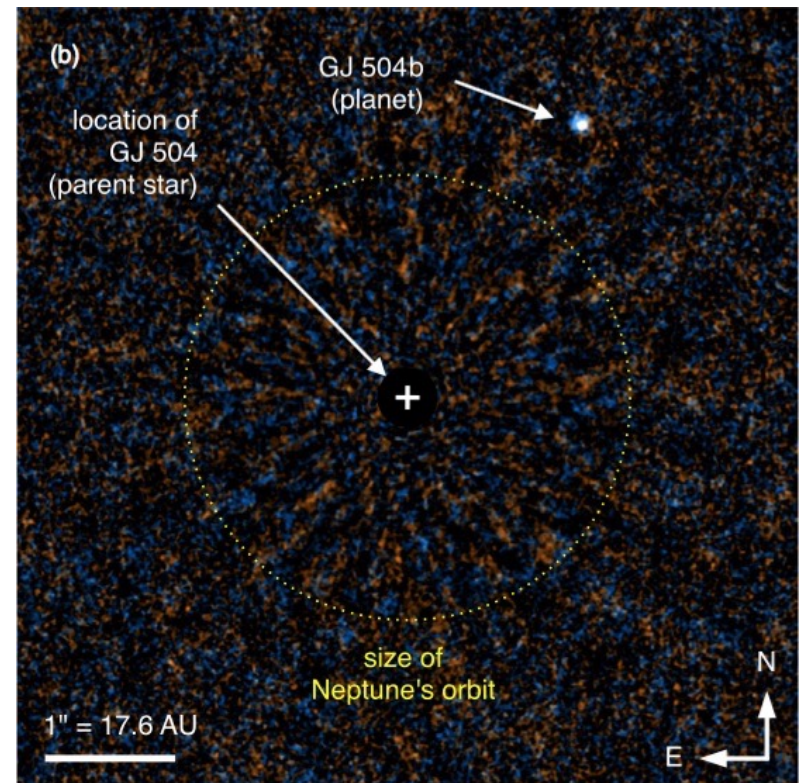Sun-like star GJ 504

$d = 17.6$ pc

Equilibrium temperature = 510 K

Adaptive optics, occulting mask, near infrared
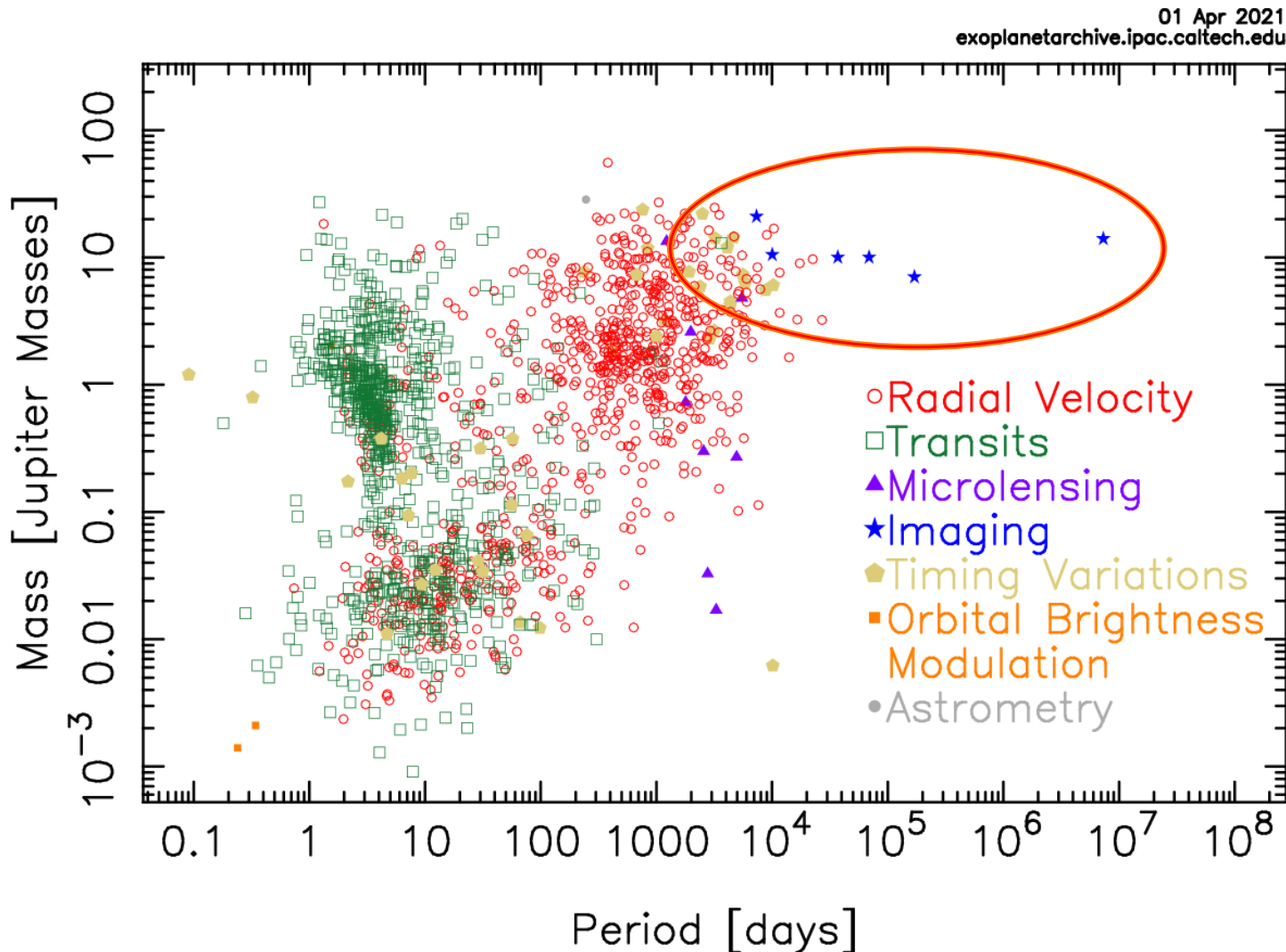
Kuzuhara et al. (2013)

Direct imaging: summary of results (2021)

Current number of confirmed exoplanets: 146 in 106 planetary systems (5 multiple)

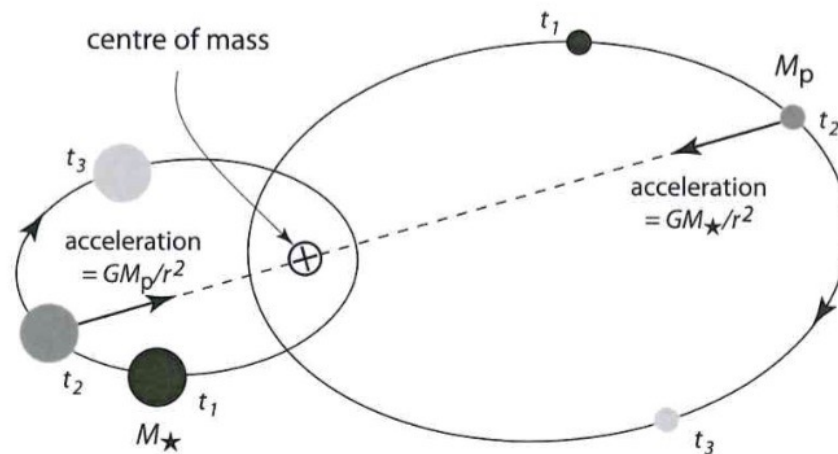These planets are quite massive and distant from the central star.

Mass – Period Distribution

01 Apr 2021
exoplanetarchive.ipac.caltech.edu

Indirect Methods:
gravitational perturbation of the stellar motion

The star and the planet orbit around their common barycenter

   – The stellar motion, induced by the gravitational perturbation of the planet, is called "reflex motion"

centre of mass

t_1

M_p

t_2

acceleration $= GM_\star/r^2$

t_3

acceleration $= GM_p/r^2$

t_2

t_1

$M_\star$

t_3

Exercise:

show that the Jupiter-Sun barycenter lies outside the volume of the Sun,

by 7% of the Sun's radius

Indirect Methods:
gravitational perturbation of the stellar motion

$$a_* = a \, \frac{M_p}{M_*}$$

The reflex motion of the star is proportional to M_p/M_*

This introduces an observational bias

that favours the detection of massive planets around low-mass stars

Indirect methods based on the perturbation of the stellar motion:

Radial Velocity (or Doppler)

Timing

Astrometric

Detection of exoplanets:
Geometric configuration of the observation

We call i the angle between the orbital spin and the line of sight
(i.e., the angle between the orbital plane and the plane of the sky)

$$i = 0^o \rightarrow \text{ face on}$$

$$i = 90^o \rightarrow \text{ edge on}$$

With this convention, the velocity vector of the motion of the central star in the orbital plane is projected along the line of sight with a factor $\sin i$

$$v_R = v \sin i$$

Earth

Line of sight

Center of mass

Star

v

v_R

i

Orbital plane

Plane of the sky
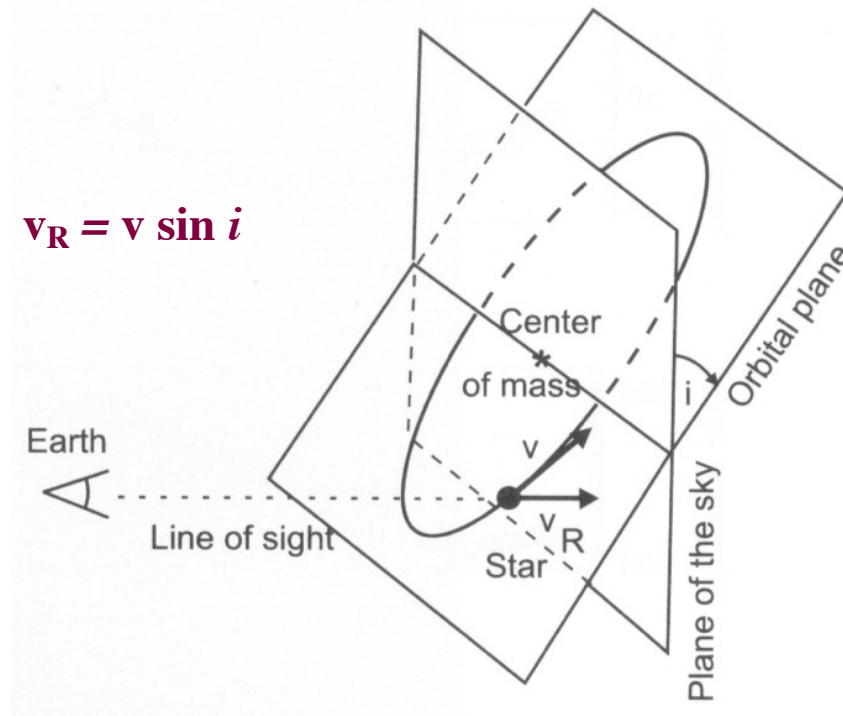
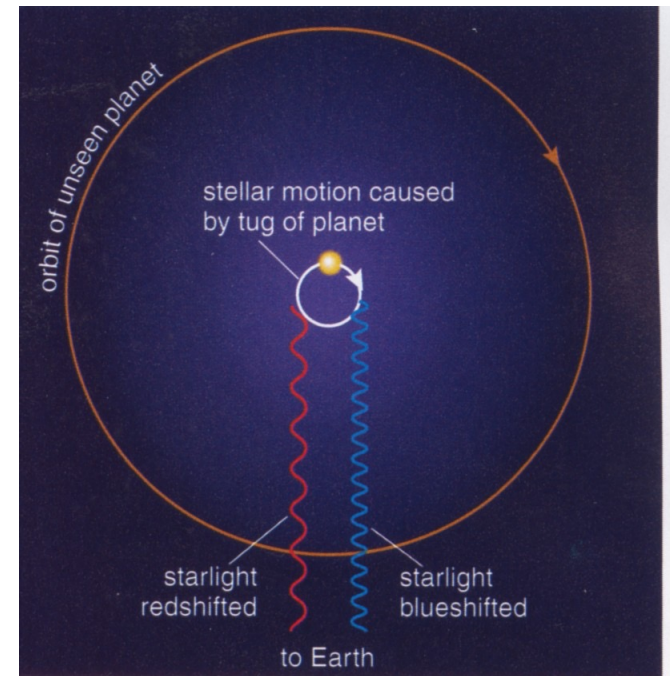# Radial velocity (or Doppler) method

Spectroscopic measurement

– Based on the measurement of the radial velocity of the stellar reflex motion at different epochs

The stellar radial velocity contains a variable term, $V_* \sin i$, due to the projection of the reflex motion along the line of sight

Thanks to the Doppler effect, the variable term $V_* \sin$ induces a periodic shift of the photospheric lines of the stellar spectrum

Requires:

high resolution spectroscopy

accurate and stable wavelength calibration

orbit of unseen planet

stellar motion caused by tug of planet
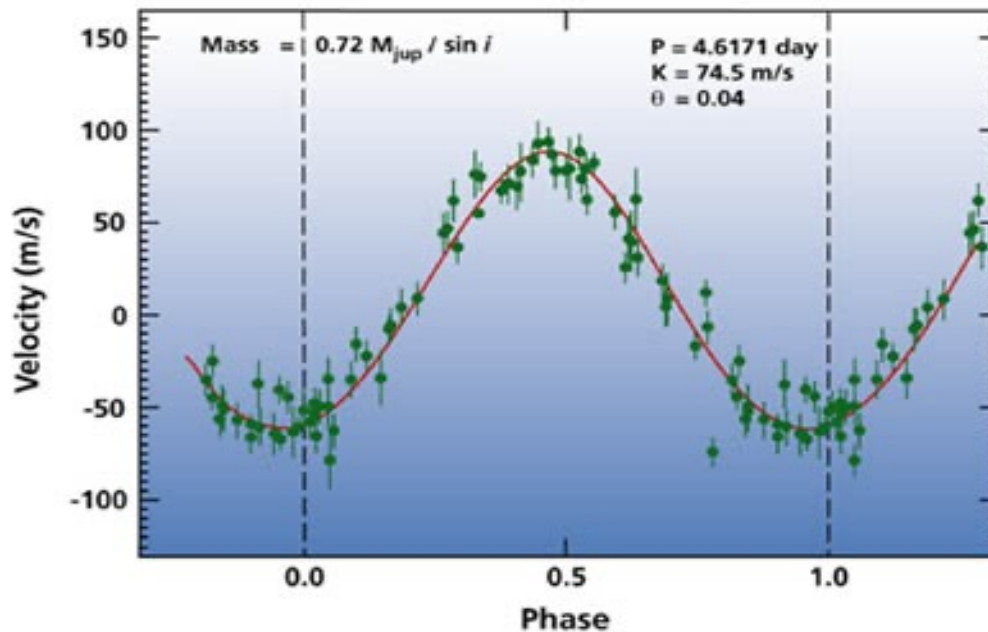
starlight redshifted

starlight blueshifted

to Earth

$$\Delta\lambda = \lambda_{\text{obs}} - \lambda_{\text{em}}$$

$$v_r \simeq \left(\frac{\Delta\lambda}{\lambda_{\text{em}}}\right) c$$

Radial velocity curves

- By plotting the stellar radial velocity as a function of time we build a radial velocity curve
- Once the periodicity is determined, data taken at different epochs can be rescaled as a function of orbital phase
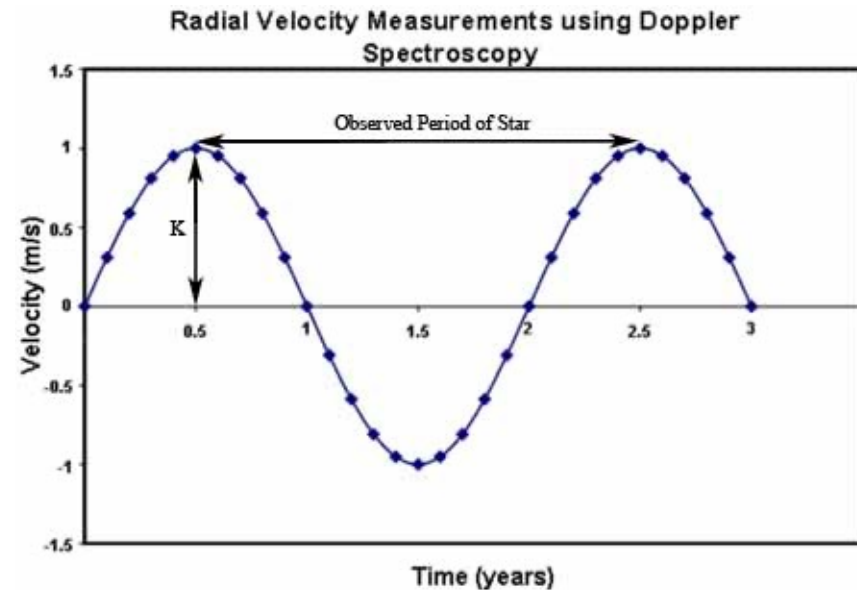

Radial velocity curve of 51 Peg b,
the first exoplanet detected with the Doppler method (Mayor et al. 1995)

Parameters that can be derived from the radial velocity curve

– Semi-amplitude, K, and period, P

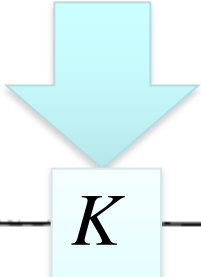The amplitude corresponds to the variation of $V_* \sin i$ during one orbital period

– The semi-amplitude is given by

$$K = \left(\frac{2\pi G}{P}\right)^{1/3} \frac{M_p \sin i}{(M_\star + M_p)^{2/3}} \frac{1}{(1 - e^2)^{1/2}}$$

Semiamplitude *K* of the solar reflex motion induced by the planets of the Solar System

W. D. COCHRAN AND A. P. HATZES

Table I
Radial Velocity Signals of the Planets

Planet	M_p (M_J)	R (AU)	P (years)	$\Theta_\star$ at 10 pc (mas)	K (ms^{-1})
Mercury	1.74E-4	0.387	0.241	6.4E-6	0.008
Venus	2.56E-3	0.723	0.615	1.8E-4	0.086
Earth	3.15E-3	1.000	1.000	3.0E-4	0.089
Mars	3.38E-4	1.524	1.881	4.9E-5	0.008
Jupiter	1.0	5.203	11.86	0.497	12.4
Saturn	0.299	9.54	29.46	0.273	2.75
Uranus	0.046	19.18	84.01	0.084	0.297
Neptune	0.054	30.06	164.8	0.156	0.281
Pluto	6.3E-6	39.44	247.7	2.4E-5	3E-5

Derivation of orbital and planetary parameters with the Doppler method

- The radial velocity curves provides the period, P, from which the semimajor axis a is inferred using the third Kepler's law

$$P^2 = \frac{4\,\pi^2\,a^3}{G\,(M_* + M_{\mathrm{p}})}$$

- The mass of the star is derived from a spectroscopic study combined with a model of stellar structure
- By fitting the radial velocity curve one can obtain the eccentricity, e, and the argument of the pericenter, ω
- In this way, from the semiamplitude K one can infer <u>a lower limit on the planet mass</u>

$$M_p \sin i = K \left(\frac{P}{2\pi G}\right)^{1/3} (M_\star + M_{\mathrm{p}})^{2/3} (1 - e^2)^{1/2}$$

Doppler method: selection effects

The limited <u>temporal baseline of the observations</u> favours detections of planets with relatively short orbital periods (i.e., small semimajor axis)

    This is true for all indirect methods of exoplanet observations

For a given stellar mass, the <u>amplitude of the reflex motion</u> scales as $M_{\mathrm{p}} P^{-1/3}$

    Easier to detect <u>massive planets with short orbital period</u> (i.e., small semimajor axis)

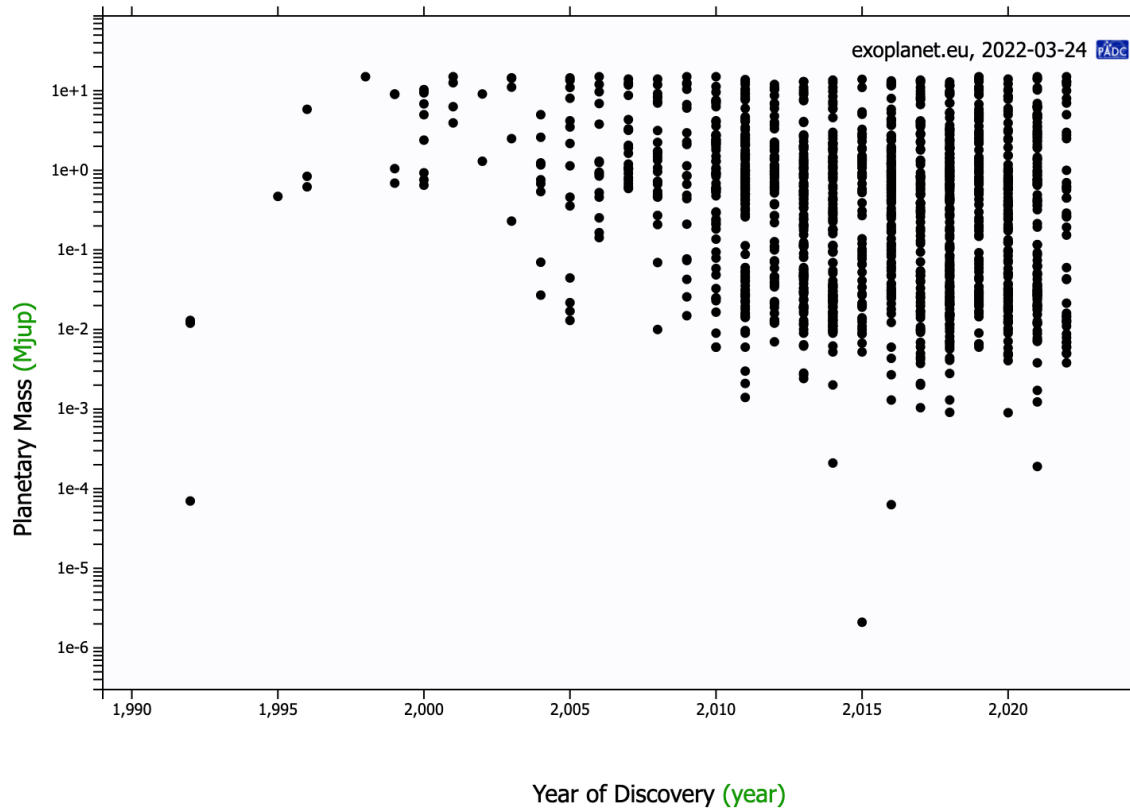For a given planetary mass, the amplitude of the reflex motion scales as $M_*^{-2/3}$

    Easier to detect <u>planets around low-mass stars</u> (e.g. M type stars)
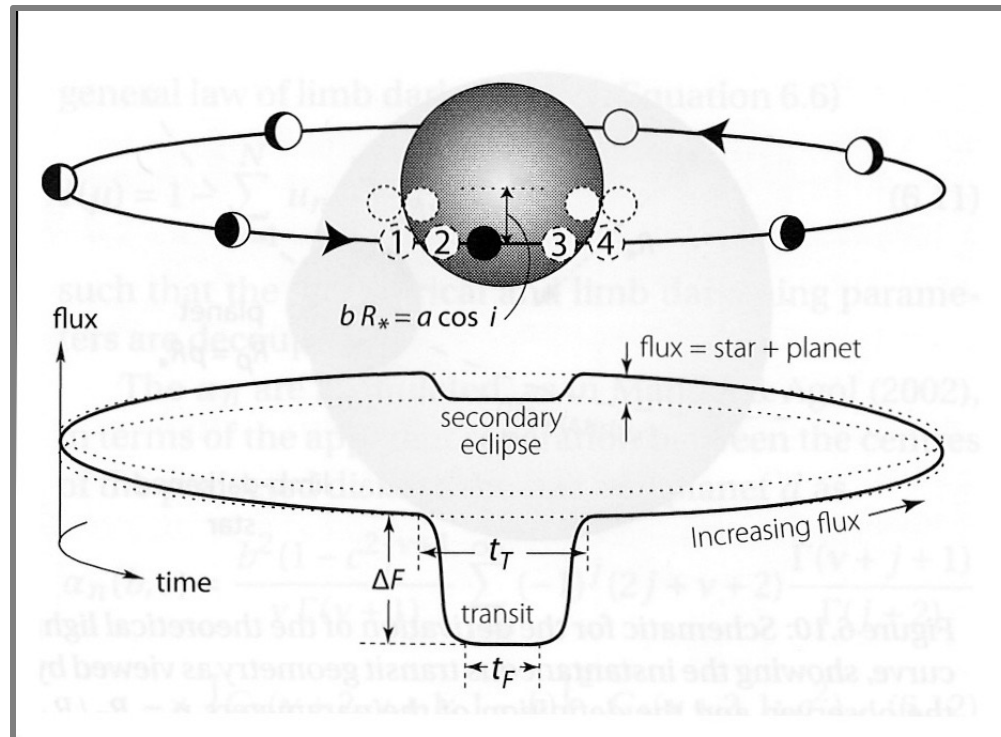
Doppler method

➢ **Very effective**

– Between 1995 and 2012 most exoplanets have been discovered with the Doppler method

– Currently (2022):

991 planets / 737 planetary systems / 174 multiple planetary systems

Transit method

If the line of sight is aligned with the orbital plane, the planet will produce a minimum in the light curve during its transit in front of the stellar disk

The stellar light curve will show a characteristic periodic behaviour

Geometric configuration: $i \approx 90^{\circ}$

Transit method

Central depth of the light profile

- Neglecting the flux emitted by the planet and limb darkening effects, the depth of the profile is:

$$\Delta F_r \cong (F - F_{tr}) / F = (R_p/R_*)^2$$

  F: stellar flux outside the transit

  F_{tr}: stellar flux during the transit (minimum of the light curve)

  R_p: planet radius

  R_*: stellar radius

- One can derive the <u>planet radius in units of the stellar radius</u>

Transit method

➢ Geometric probability

- The geometric probability of detecting a planet with the transit method is proportional to R_*/a

  R_*: stellar radius; a: orbital semi-major axis

  Typical value of the geometric probability:

  $p_{\mathrm{geom}} \sim 0.0045 \, (1 \text{ AU}/a) \, (R_*/R_\odot)$

  Charbonneau et al. (2007)

➢ Time probability

- The probability of observing a transit at any given time scales with t_T/P, where t_T is the duration of the transit phase

  For an Earth-type orbit ~ 13 h/365 d ~ 0.001

Transit method

Selection effects

   – The transit signal increases with $(R_\mathrm{p}/R_*)^2$

      Easier to find large planets orbiting small stars

   – Number of detections biased by the geometrical probability $p_\mathrm{geom} \sim R_*/a$

      Easier to find planets with small semi-major axis (short periods)

      Extremely difficult to find planets at distances larger di 5 - 10 AU

      The selection effect of small semi-major axis reinforces the effect due to the temporal baseline of the observations, which favours detections of planets with short orbital periods

      Relatively easy to find giant planets close to the host star
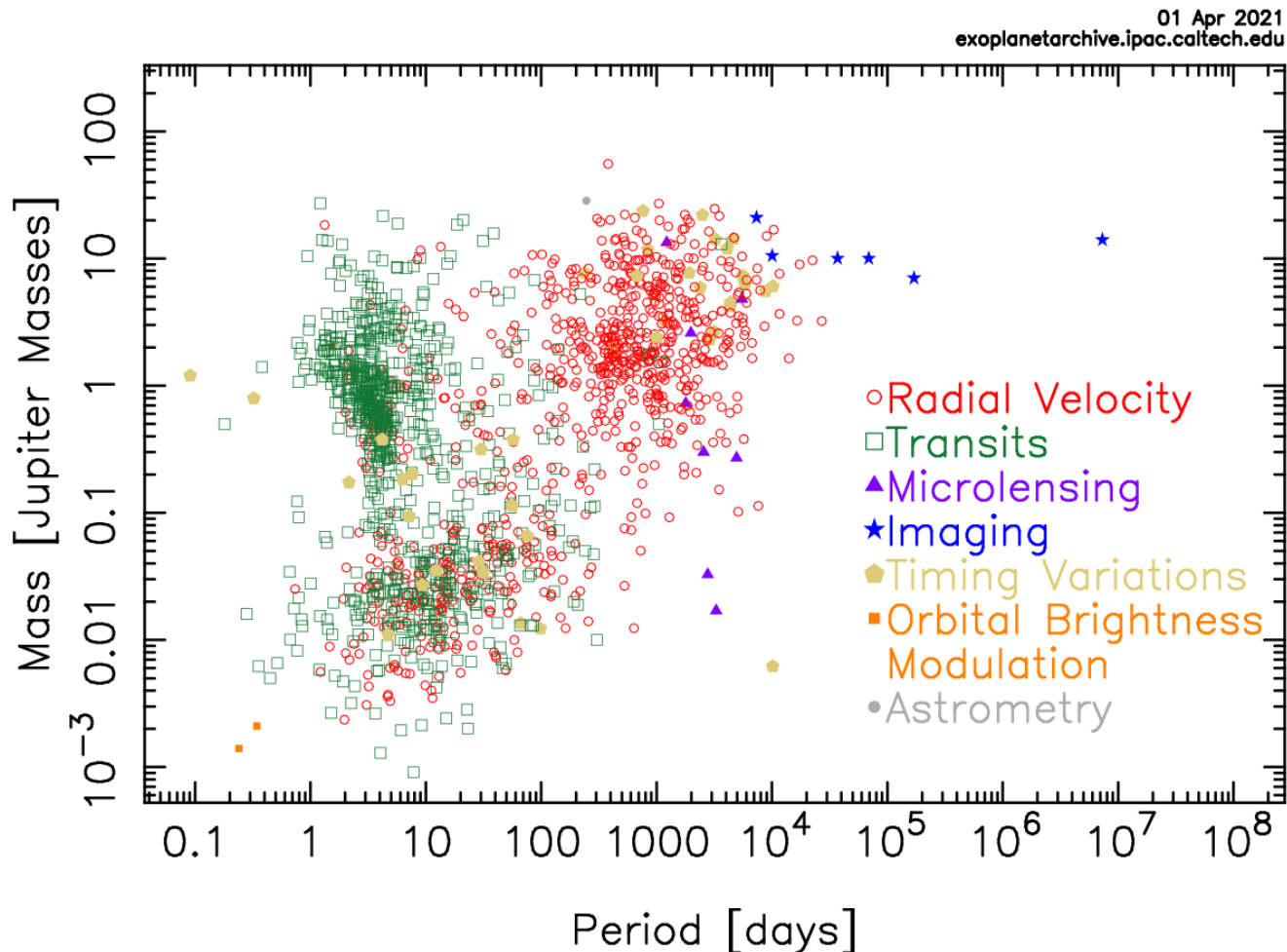   as an example, "hot-Jupiters"

Transit method: summary of results (2021)

So far, discovered 3414 planets in 2563 planetary systems

553 multiple planetary systems

Broad ranges of planetary masses, but the number drops with increasing period

Mass − Period Distribution

Exoplanets characterization

Study of the physical properties of individual planets

- – Direct imaging can provide data useful to characterize individual planets, but feasible only for a small number of cases
- – In general, the best way to constrain the properties of individual exoplanets is to combine different observational techniques
- – From this combination of experimental data, with the aid of modelization, we can derive information on

    Planetary interiors

    Planetary atmospheres

    Planetary energy budget

Planets with measurements of masses and radii

– From mass and radius measurement we obtain

– <u>mean density</u> $\varrho \sim M/R^3$

  Casts light on the internal structure/composition of the planet

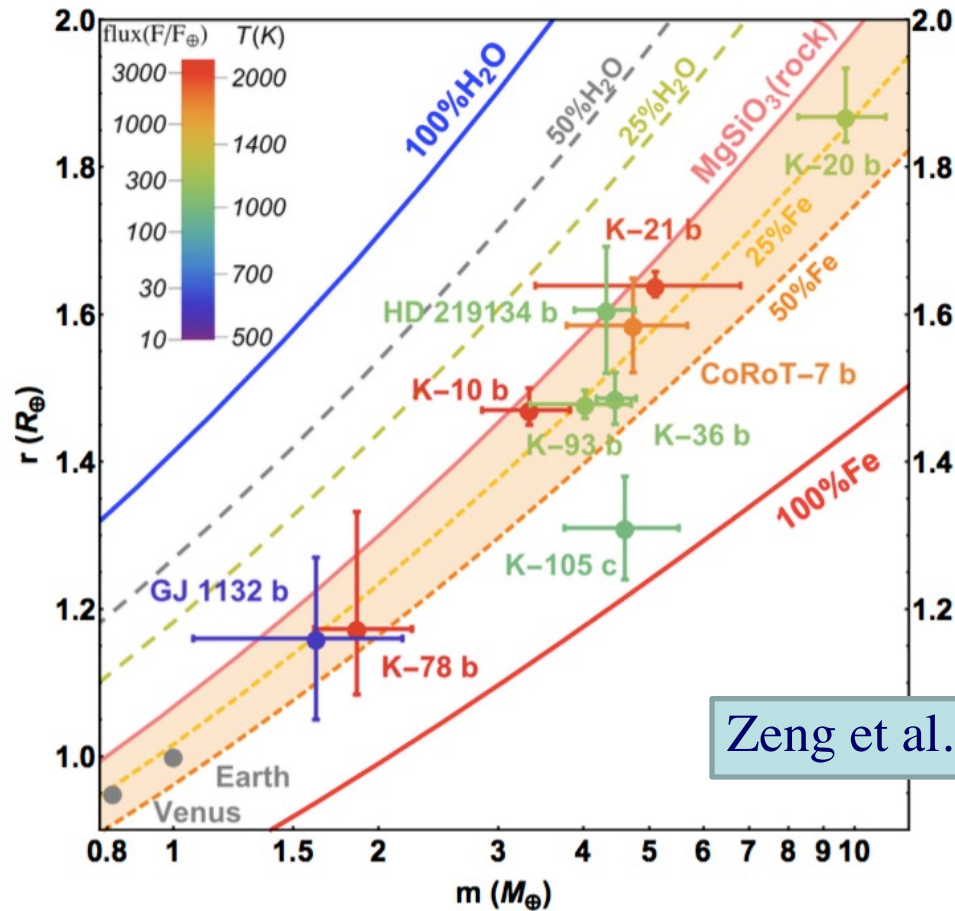– <u>surface gravity</u> $g \sim M/R^2$

  Important for the modelization of the atmosphere and climate

– <u>escape velocity</u> $v_e \sim (M/R)^{1/2}$

 Indicates the capacity for the planet to maintain an atmosphere

Mass versus radius: comparison with models of planetary interiors

Zeng et al. (2017)

Mass-radius plots showing selected rocky planets
Curves show models with different compositions
Planets are color coded according to their incident stellar flux

Mass versus radius: casting light on the process of planetary formation

Weiss & Marcy (2014)
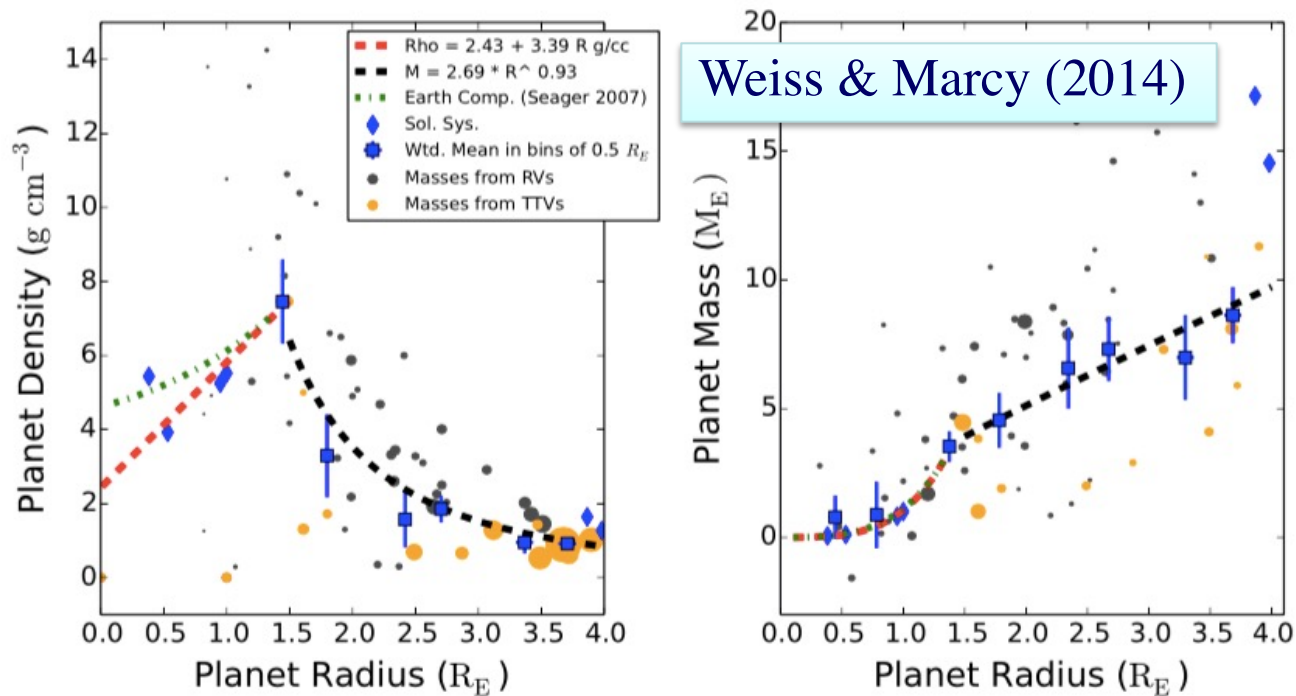
Figure 2. Left: density vs. radius for 65 exoplanets. Gray points have RV-determined masses, orange points have TTV-determined masses, and the point size corresponds to $1/\sigma(\rho_P)$. The blue squares are weighted mean densities in bins of $0.5\,R_\oplus$, with error bars representing $\sigma_i/\sqrt{N_i}$, where σ_i is the standard deviation of the densities and N_i is the number of exoplanets in bin i. We omit the weighted mean densities below $1.0\,R_\oplus$ because the scatter in planet densities is so large that the error bars span the range of physical densities (0–10 g cm^{-3}). The blue diamonds indicate solar system planets. The red line is an empirical density–radius fit for planets smaller than $1.5\,R_\oplus$, including the terrestrial solar system planets. The green line is the mass–radius relation from Seager et al. (2007) for planets of Earth composition (67.5% $MgSiO_3$, 32.5% Fe). The increase in planet density with radius for $R_P < 1.5\,R_\oplus$ is consistent with a population of rocky planets. Above $1.5\,R_\oplus$, planet density decreases with planet radius, indicating that as planet radius increases, so does the fraction of gas. Right: mass vs. radius for 65 exoplanets. Same as left, but the point size corresponds to $1/\sigma(M_P)$ and the blue squares are the weighted mean masses in bins of $0.5R_\oplus$, with error bars representing $\sigma_i/\sqrt{N_i}$, where σ_i is the standard deviation of the masses and N_i is the number of exoplanets in bin i. The black line is an empirical fit to the masses and radii above $1.5\,R_\oplus$; see Equation (3). The weighted mean masses were not used in calculating the fit. Some mass and density outliers are excluded from these plots, but are included in the fits.

Statistical properties of exoplanets
Distribution of planetary masses and radii

- – *M* sin *i* distribution obtained with the Doppler method

The distribution increases towards values of low mass

 - – Despite the selection effect that favours the detection of high mass planets

 - – Once corrected for selection effects, also the distribution of radii indicates that small-size planets are more frequent than large planets
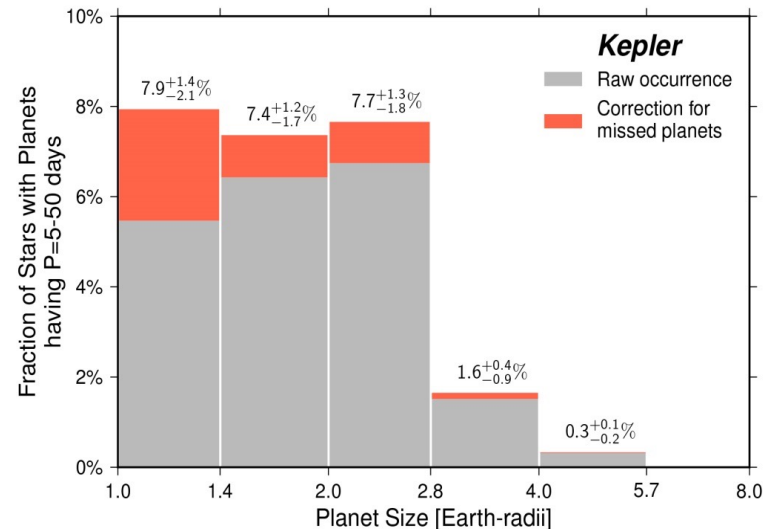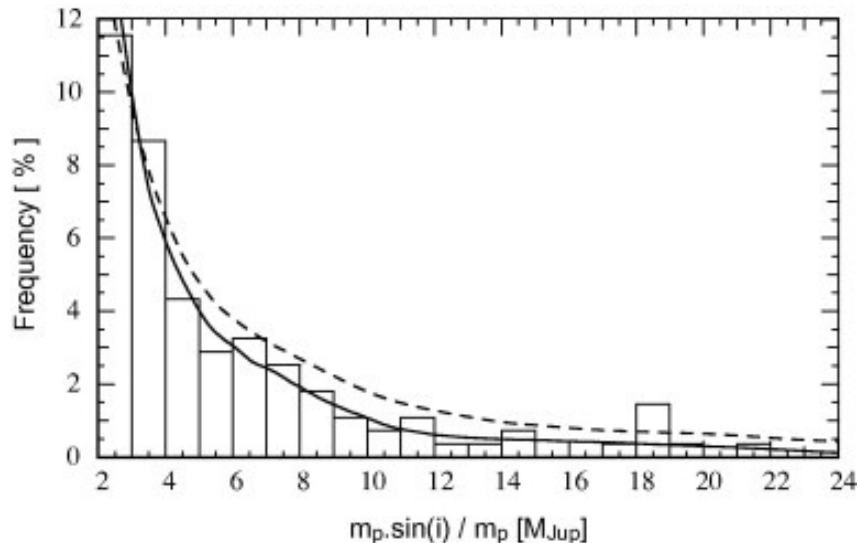
Frequency of exoplanet detection vs. metallicity of the host star:
Trends for different planetary radii

(Buchhave et al. 2012)

R<4R$_{Earth}$

R>4R$_{Earth}$